Journal of Molecular Graphics and Modelling 27 (2009) 744–750

Contents lists available at ScienceDirect

Journal of Molecular Graphics and Modelling

journal homepage: www.elsevier.com/locate/JMGM

Computational analysis of R and S isoforms of 12-Lipoxygenases: Homology modeling and docking studies

P. Aparoy [a], T. Leela [a], R.N. Reddy [b], P. Reddanna [a,*]

[a] School of Life Sciences, University of Hyderabad, Hyderabad 500046, India
[b] Rational Labs (P) Limited, Plot #177, IDA Mallapur, Hyderabad 500076, India

ARTICLE INFO

Article history:
Received 10 August 2008
Received in revised form 18 November 2008
Accepted 19 November 2008
Available online 27 November 2008

Keywords:
Lipoxygenase
12R-LOX
12S-LOX
15-Lipoxygenase
Homology modeling
Molecular docking

ABSTRACT

The present study is aimed at predicting human 12R-LOX structure by constructing a homology model. Based upon Blast results, rabbit reticulocyte 15-Lipoxygenase 1LOX (protein data bank) was considered as a template for homology modeling. The 3D model was generated with Modeler in InsightII and further refined using AMBER. Further to understand the relationship of protein structure with stereo specificity, a comparative analysis of 12R-LOX model was done with that of 12S-LOX homology model to identify differences in the binding site topology and interacting residues. The large insertion of 31-aa seen in 12R-LOX is located beyond the N-terminal barrel and is accommodated on the outside of the protein without disruption of the overall tertiary structure. The 31-aa region includes SH3 domain binding PXXP motif, seven prolines and five arginines. The docking of the substrate, arachidonic acid was also performed. Our results show that the Gly441 and substrate orientation within the active site play an important role in stereo specificity of 12R-LOX.

1. Introduction

Lipoxygenases (LOXs) are a group of structurally related family of non-heme, iron-containing dioxygenases [1]. LOXs are widely distributed in numerous eukaroyotes, and recently found to be present in bacteria [2]. LOXs infer regio (positional) specificity because of incorporation of molecular oxygen at different positions on the substrate fatty acids and thus are classified as 5-, 8-, 12-, and 15-LOXs in animals and 9- and 13-LOXs in plants [2,3]. Based on stereo specificity of oxygen insertion, they are characterized as R and S LOXs [3]. Till now, five human LOXs have been identified; 5-LOX [4,5], 12-LOX [6,7], 12R-LOX [8], 15-LOX (15-LOXa) and 15S-LOX (15-LOXb) [9–11]. LOXs are versatile catalysts as they are multifunctional enzymes catalyzing different types of reactions. 5-LOX is mainly responsible for the synthesis of a number of inflammatory mediators, including leukotrienes, which mediate inflammatory disorders such as bronchial asthma [12]. Products of 12R-LOX are associated with various skin diseases [8] and 15-LOX products are associated with atherosclerosis [13]. Lipoxygenase metabolites have also been implicated in a number of non-inflammatory biological processes. e.g.: 12-HETE and 15-HETE have been implicated in tumour metastasis and in the formation of atherosclerotic plaques, respectively [8,13].

12R-hydroperoxyicosatetraenoic acid (12R-HPETE), a product of 12R-LOX, is involved in psoriasis and promotes the proliferation of colon cancer cells *in vitro* [14–16]. Initially it was thought that the product 12R-HETE was formed only from cytochrome P450, later it was proved that this was also formed from 12R-LOX, which has been cloned from human skin [8]. Generally most of the LOXs act on free PUFAs [8], but only in humans, 12R-LOX acts on both free and bound fatty acids. 12R-LOX was first cloned in human keratinocytes and psoriatic scales [15]. This provides an additional target for potential therapeutic interventions for psoriasis and other non-psoriatic acute dermatitis. The inhibition of human 12R-LOX activity is of considerable interest in treatment of psoriasis and other skin cancers. 12R-lipoxygenase or epidermal lipoxygenase-3 (eLOX3) function together in the normal process of skin differentiation, and that the loss of function mutations is the basis of the LOX-dependent form of non-bullous congenital ichthyosiform erythroderma (NCIE) [17,18].

Specificity in the formation of products and regulation in the members of the LOXs family emphasize the importance of LOX structure and its active site residues. Generally LOXs belong to a family of structurally related proteins. Despite the low sequence similarity among different LOXs, these proteins show a common structural fold. The overall LOX fold consists of an N-terminal eight-stranded antiparallel β-barrel domain and the larger catalytic domain formed predominantly by α-helices. The main catalytic domain of LOX enzymes contains a single non-heme iron held in place by a conserved group of amino acid ligands,

* Corresponding author. Tel.: +91 40 23134542; fax: +91 40 23010745.
E-mail addresses: prsl@uohyd.ernet.in, preddanna@yahoo.com (P. Reddanna).

1093-3263/$ – see front matter © 2008 Elsevier Inc. All rights reserved.
doi:10.1016/j.jmgm.2008.11.009

predominantly histidines plus the C-terminal carboxyl group of the polypeptide i.e. terminal Isoleucine [19,20]. Based on sequence alignments it is clear that this center of catalysis is of very similar structure throughout the LOX gene family. The similarity is even higher in the catalytic domain in the region of the active site, with the iron ligands almost super-imposable. The iron ligands are in an octahedral arrangement with one position unoccupied and with sufficient space for substrate/inhibitor binding [21]. Currently, there are no LOX structures available with bound substrate, and, given the inherent flexibility of fatty acid carbon chains, this leaves many uncertainties associated with the positioning of the substrate during catalysis [22]. R-LOXs, similar to S-LOXs contain the same conserved motifs and iron ligands. The sequence motif that accounts for the stereo specificity was not known. The change in reaction specificity must be capable of giving narrow range products. Site-directed mutagenesis studies around active site residues have identified a candidate residue involved in the stereo specificity. Ala that is conserved in all S-LOXs is replaced by Gly in R-LOXs [23]. Ala in S-LOXs promotes oxygenation on the reactive pentadiene at the substrate-binding pocket whereas Gly in R-LOXs promotes oxygenation on proximal position of reactive pentadiene [23]. The key elements for positional and stereo specificity, depend on the depth of the substrate that enters into the catalytic domain of the protein and head to tail orientation of the substrate [23–25]. In different LOX enzymes, no doubt the active sites have modifications to effect specific reactions, but with the basic enzyme structure conserved, it is re-alignment of substrate that permits the range of specific oxygenations found within the LOX gene family. Reversed substrate orientation and frameshift repositioning are key to this flexibility.

To date, structural information for only three lipoxygenases is available from the Protein Data Bank of Brookhaven (PDB, www.rcsb.org/pdb): two isoforms from soybeans, LOX-1 and LOX-3, and one from rabbit reticulocytes, 15-LOX. Homology modeling technique has been recently used in the generation of reasonable 3D model of various lipoxygenases which were in turn successfully used in various structure based drug design strategies [26–28]. The Human 12R-LOX which shows pure R-stereo chemistry has been recently reported and the crystal structure is yet to be elucidated. In the present investigation, the 3D structure of 12R-LOX is constructed theoretically by taking the crystal structure of rabbit reticulocyte 15-LOX [29] as template. The 3D model of 12R-LOX is used to search the active site and carry out the binding studies with the substrate, arachidonic acid. Further to understand the relationship of protein structure with stereo specificity, a comparative analysis of 12R-LOX model was done with that of 12S-LOX homology model to identify differences in the binding site topology and interacting residues, which might be utilized to develop selective 12R-LOX inhibitors.

2. Methodology

All molecular simulations were performed on the SGI workstation by using InsightII software from Accelrys, USA [30]. The amino acid sequence of 12R-LOX (Accession Id: AAC39770) was obtained from the databank in the National Center for Biotechnology Information, NCBI (www.ncbi.nlm.nih.gov). The BLAST program against Protein Data Bank (PDB) available at NCBI was used to select a template structure for homology modeling of 12R-LOX. The crystal structure of rabbit reticulocyte 15-LOX (PDB code: 1LOX) was obtained from PDB database [31] and it shares 33% sequence identity with 12R-LOX as shown in Fig. 1. The first requirement in the construction of 12R-LOX model is the sequence alignment among these templates. The sequence alignment is based on identifying structurally conserved regions (SCR) common to the template and target. The alignment from ClustalW program was used to build the initial model. To construct the protein model for the target sequence, we used the InsightII/Homology program [32] implemented on a Silicon Graphics workstation. Ten models were generated and the model showing the least rms deviation with respect to trace (Cα atoms) of the crystal structure of the template, 15-LOX was saved for further refinement and validation. Further, refinement was performed in order to obtain the best conformation of 12R-LOX structure resulting from Modeler. Iron atom was added to the model in InsightII and it is ligated to three histidines, His398, His403, His578, Asn582 and Ile701.

The protein model was energy minimized using AMBER 3.0 [33]. A four-stage protocol was established for energy minimization of the solvated protein [34]. These minimizations were carried out using periodic boundary conditions in all directions and each stage involved 100 steps of steepest descent and 1500 steps of conjugate gradient optimization. In the first stage of minimization, only the solvent molecules were minimized keeping the protein fixed. In the second stage, both solvent and hydrogen atoms in the protein were allowed to relax while keeping the heavy atoms of the protein fixed. In the third stage, backbone atoms of the protein were fixed, while allowing the solvent and the side chains of the protein to move during optimization. In the fourth stage all the solvent molecules and the protein atoms were allowed to relax.

The quality of the refined 12R-LOX structure obtained was checked with Profile-3D. The Profile-3D tests the validity of hypothetical protein structures by measuring the compatibility of the hypothetical structure with its own amino acid sequence [35]. To verify the protein model, the coordinates of the protein model were submitted to PROCHECK [36]. The stereochemical quality of the protein structures is examined by a Ramachandran plot using the PROCHECK program, the number of residues that are in the allowed or disallowed regions of Ramachandran plot determines the quality of the model. The root mean square deviation (RMSD) of the model with respect to Cα atoms of the template was measured using the Combinatorial Extension (CE) method [37]. In this study, the CASTp server was used for the identification of the main binding site in 12R-LOX. CASTp provides identification and analytical measurements of surface accessible pockets, for proteins and other molecules, which can be used to guide protein–protein interactions [38]. We can predict the main binding site of 12R-LOX through comparison of the reported structures of 15-LOX, Soybean LOX-1 and Soybean LOX-3.

In order to make an attempt to understand R or S stereo specificities, we searched for conserved differences between R and S lipoxygenases in residues in and around the active site. A homology model of 12S-LOX (Accession no. NP_000688) was also built using the same methodology as described above. The structure of rabbit reticulocyte 15-LOX [26] was selected as template to generate the model due to its high sequence identity of 61% with that of 12S-LOX.

GOLD (Genetic Optimization of Ligand Docking), a docking program based on genetic algorithm [39] was used to dock the substrate i.e. arachidonic acid. The structure of arachidonic acid was sketched and minimized using cerius2 and structure with cis double bonds is obtained in conformational analysis. Based on the superimposition of the template, rabbit reticulocyte 15-LOX with the 12R-LOX and 12S-LOX 3D structures, active site was defined as a sphere of 10 Å centered on the inhibitor in the template. During docking, the default algorithm was selected. Input parameters of the GOLD were set to allow octahedral coordination geometry to iron. The number of poses for each inhibitor was set to 100, and early termination was allowed if the top three bound conformations of a ligand were within 1.5 Å RMSD. After docking, the individual binding poses of each ligand were observed and their interactions with the protein were studied. The best and the most energetically favorable conformation of each ligand was selected.

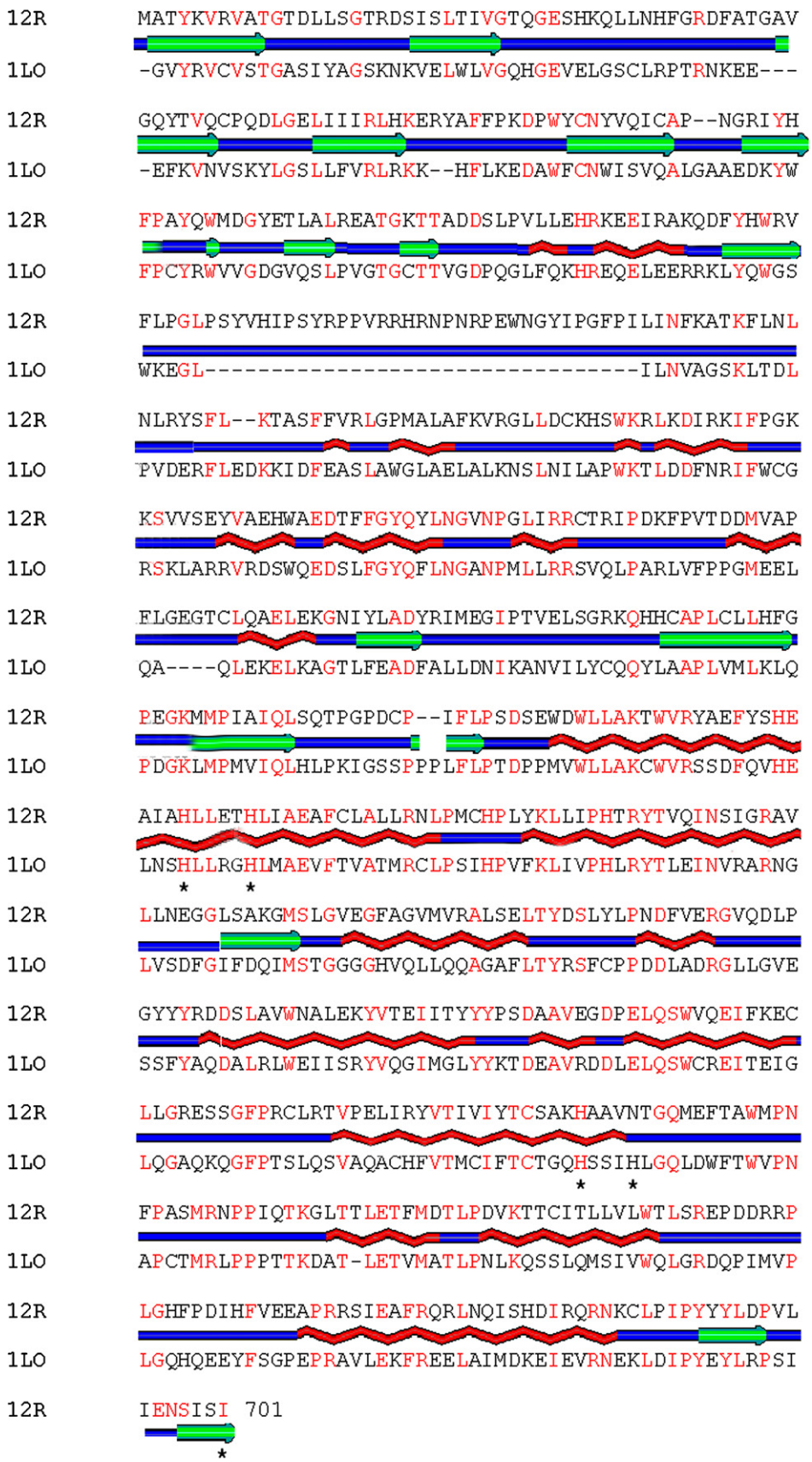

Fig. 1. Sequence alignment of the query, 12R-Lipoxygenase with the template, 1LOX, rabbit reticulocyte 15-LOX using ClustalW [35]. Identical residues are shown in red, while the iron-binding residues are denoted by asterisk (*). The line between sequences shows the secondary structure, as determined by the SABLE server (http://sable.cchmc.org/). Green arrows represent β-strands, α-helix is shown in red and the blue line represents the loops.

A four-stage protocol was set up for energy minimizations of the protein–inhibitor complex using AMBER [33]. Minimization at each stage was performed using 200 steps of steepest descent and 1500 steps of conjugate gradient algorithms for minimization. In the first stage, only the solvent molecules were minimized, keeping the inhibitor and the protein (in the complex calculation) fixed. The purpose of this step is to relieve any bad contacts involving solvent molecules in the initially solvated system. In the second stage, only hydrogens in the system were allowed to relax. This step relaxes the hydrogen atoms prior to relaxing heavy atoms. It was performed because the adjustments in hydrogen atom locations are necessary to improve hydrogen bond geometries. In the third stage, all atoms of the protein were fixed, while allowing all the atoms of the inhibitor and the solvent to move during optimization. This stage allows for the relaxation of the inhibitor with respect to the protein and establishes the preferred interactions (e.g., hydrogen bonds). In the fourth and final stage, all the atoms of residues within 15 Å from the center of the inhibitor (solvent molecules, protein atoms and the ligand) were allowed to relax. After four-stage protocol energy minimizations, the optimized structures of protein and ligand were visualized and studied using InsightII.

3. Results

The search for the best template for modeling of 12R and 12S-LOXs was carried out using PSI-BLAST against PDB. The rabbit reticulocyte 15-LOX (PDB id. 1LOX) proved to have the best sequence similarity with both the 12R and 12S lipoxygenases. Beyond the highest sequence similarity it also showed the higher sequence identity. The sequence alignment of template Rabbit 1LOX sequence showed 33.4% identity and 52.7% similarity with human 12R-LOX sequence, 61% identity and 77% of similarity with human 12S-lipoxygenase (Fig. 1). Even though the identity of 12R-LOX with the template is low when compared to 12S-LOX the knowledge of amino acids involved with stereo specificity, positional specificity and catalytic residues of lipoxygenases was helpful in the construction of a reliable model. The alignment of 12R-LOX with 1LOX showed that the residues are mainly conserved at iron-binding residues and at the catalytic domain. The main differences were observed only at N-terminal sequence; a large proline rich insertion is present at the start of the C-terminal domain of 12R-LOX. As the catalytic domain is present in the C-terminal domain of lipoxygenases, these insertions may not affect the catalytic activity. So 1LOX was selected as a template for 12R and 12S modeling studies. The initial model of 12R-LOX was generated using Modeler in InsightII. The initial model was refined using four-stage energy minimization protocol in AMBER. The refined models were then validated for their stereochemical quality (Fig. 2) and side chain environment and the results are shown in Table 1.

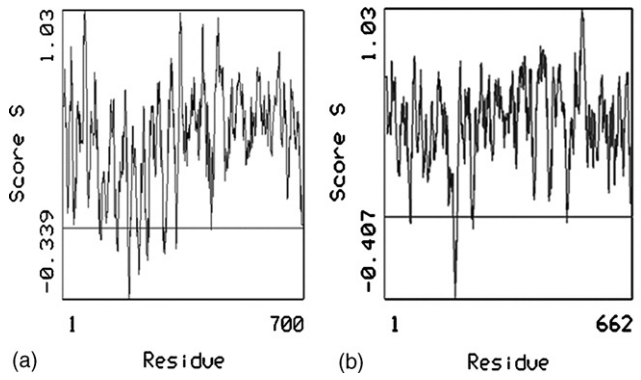

Fig. 2. Profile-3D graph of (a) 12R-LOX and (b) 12S-LOX.

Table 1
Protein structure analysis of the models obtained for 12R-LOX and 12S-LOX.

Model	12R-LOX	12S-LOX
Φ–ψ violation[a]	1.2	0.3
Verify-3D[b]	86.31	93.21
Profile-3D[c]	268.82	279.09
CE[d]	1.3 Å	0.4 Å

[a] Percentage of residues lying in the disallowed region.
[b] Percentage of total residues with averaged 3D–1D score > 0.2.
[c] The minimum and maximum possible scores for 12R model are 136.147 and 303.147, respectively. The minimum and maximum possible scores for 12S model are 144.312 and 320.694, respectively.
[d] Root mean square deviation of the backbone atoms with that of the template.

Comparison of numerous LOX amino acid sequences as well as mutagenesis studies and crystal structure analysis led to the identification of highly conserved residues [40] and important residues involved in iron chelation [41,42]. The iron atom follows the structural pattern at the active site residues that is conserved in all LOXs. It is in distorted octahedral geometry. There are five amino acid ligands, the imidazole N atoms of three histidine residues: His398, His403, His578; and carboxylate oxygen of the C-terminal isoleucine, Ile701 and the carboxyl oxygen of the amide of asparagines, Asn582 (Fig. 3). The sixth coordination position faces an open cavity that usually accommodates the substrate/inhibitor. In the case of 12S-LOX the iron-binding residues are His360, His365, His 541, His545 and Ile663. The overall folding pattern of lipoxygenases is conserved across the available 3D structures and is also recognized in the 12R-LOX and the 12S-LOX models. It is composed of two folding units; a small N-terminal β-barrel domain, suggested to interact with lipids and a larger C-terminal catalytic domain, mainly composed of α-helices, and containing the active site, i.e. iron-binding site and the substrate-binding cleft (Fig. 4). Based on the superimposition of the template, rabbit reticulocyte 15-LOX with the 12R-LOX and 12S-LOX 3D structures, active site was defined as a sphere of 10 Å centered on the inhibitor in the template, (2E)-3-(2-oct-1-yn-1-ylphenyl)acrylic acid. The knowledge of the orientation of these active site residues is

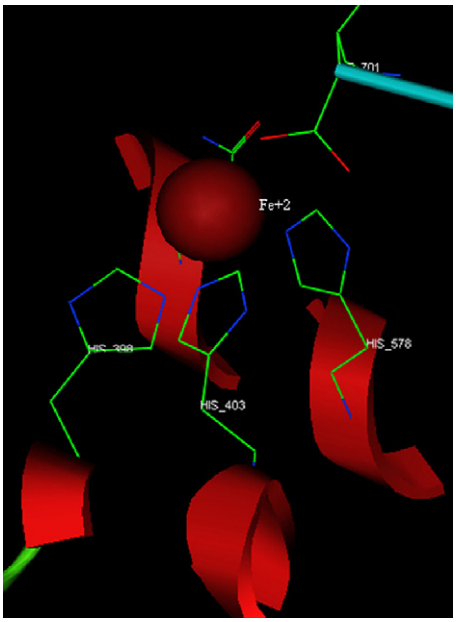

Fig. 3. Iron and its coordinates in 12R-Lipoxygenase. Iron-binding residues are three histidines, His398, His403, His578 and Ile701.

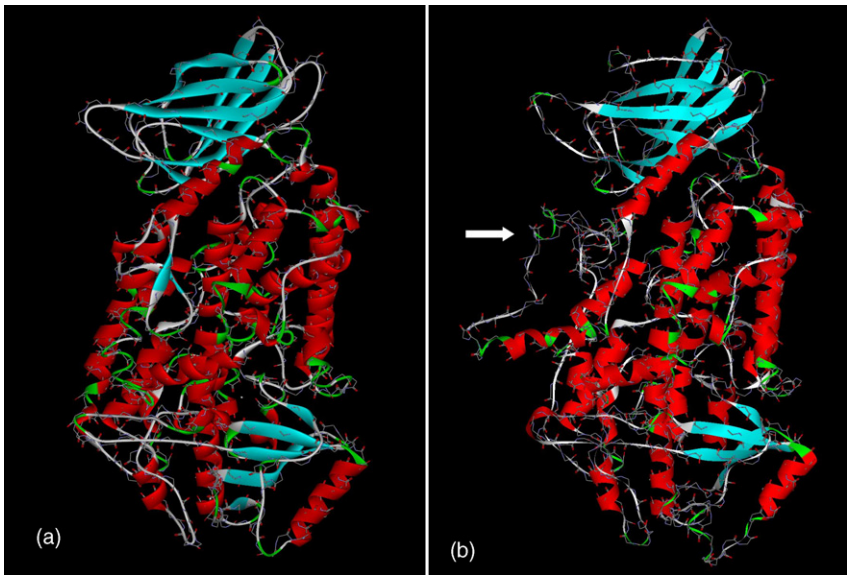

Fig. 4. Secondary structures of (a) 12S-LOX and (b) 12R-LOX. The 31-aa insert in 12R-LOX is highlighted with an arrow.

extremely useful in designing a potential inhibitor of 12R-LOX. The superposition of the generated models with crystal structure of 15-LOX shows a high similarity around the catalytic domain. CASTp server identified two major cavities; the inter domain cavity and the active site cavity.

The availability of site-directed mutagenesis data is very important for the validation of structural models with low homology between the template and the target. However, to interpret if an amino acid is directly involved in ligand binding, or structurally important by maintaining a correct structure of the binding pocket, is not straight forward [43]. We used the GOLD program for the docking studies of the substrate arachidonic acid in binding site of the 12S and 12R-LOX structures. It is observed that the substrate occupies the center of the active site cavity at the sixth coordinate position of iron. The best conformation of arachidonic acid is selected and the protein–substrate complex is visualized in DS Visualizer® (v. 1.7, Accelrys Software Inc.).

In the case of 12R-LOX, the binding cavity is lined by amino acids Leu399, His403, Ile437, Asn438, Gly441, Gly445, Ala597, Thr628, Val631 and Leu632 (Fig. 5). The Gly residue is located opposite to the non-heme iron with part of the substrate-binding cavity. This position is suitable to influence oxygenation on the side of the pentadienyl radical closer to the surface of the enzyme. In 12R-LOX, the amino acids that can be targeted for strong hydrogen bonding interactions for inhibitor design are Glu394, Glu407, Asn438, Arg442, Ser452, Leu635 and Ile701. The active site of 12R-LOX shows pocket near the Gly441 residue, which may be the potential oxygen-binding pocket. The metal atom iron is present nearer to the C10 position of Arachidonic acid. Ala403 is the corresponding residue of 12S-LOX to the Gly441 of 12R-LOX. The oxygen-binding pocket is not seen near Ala as it has methyl group. The potential oxygen-binding pocket is observed deeper in the active site possibly near to the Leu407 and Ile408 residues. Site-directed mutagenesis data on 12R-LOX confirm the involvement of Gly441 in the enantioselectivity of the enzyme [23]. Even though the active site geometry of both the enantiomers (12R and 12S-LOX) are different, still they have a common position of oxygenation on the arachidonic acid. This is very well explained by the hypothesis of head to tail orientation of the substrate proposed by Brash and co-workers [22]. In the present 12S-LOX model, the substrate with tail first (reverse orientation) was the most stable conformation. In the 12S-LOX the amino acids at the binding cavity are Lys157, Glu175, Arg171, His360, His365, Glu356, Ile357, Leu361, Glu398, Ile399, Leu597, Ala403, Leu407, Gln406, Arg402, Thr405, Ile408 and Asn400. In the 12S-LOX, the acceptor and donor atoms of Lys157, Arg171, Glu175, Glu398, Arg402 and Thr405 can be targeted for strong interactions with inhibitors.

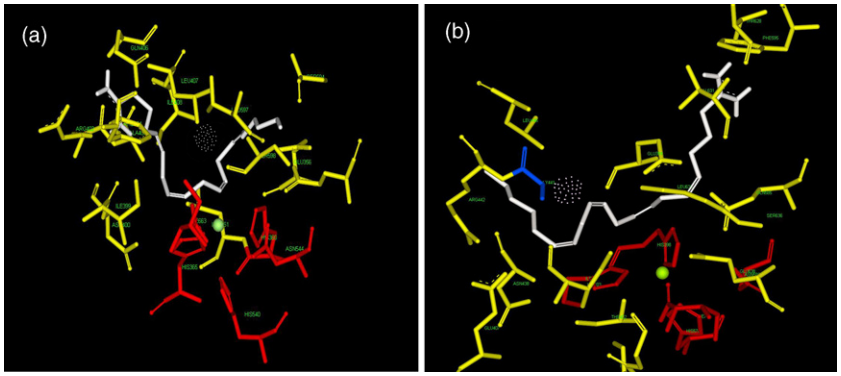

Fig. 5. (a) Substrate, arachidonic acid (white) docked in the active site (yellow) cavity of 12S-LOX. Iron is shown in green and iron ligating residues are in red colour. (b) Substrate, arachidonic acid (white) docked in the active site (yellow) cavity of 12R-LOX. Gly428 pocket is shown as dotted circle. Iron is shown in green and iron ligating residues are in red colour.

4. Discussion

12R-LOX, one of the important enzymes in the arachidonic acid metabolism, has aroused considerable interest as a major target for the discovery of antipsoriatic agents. Although various studies on 12R-LOX have been reported till date, the structural details of the enzyme are not yet known. In the present study, the 3D models of the R and S isoforms of 12-Lipoxygenase were generated based on the structure of the rabbit reticulocyte 15-Lipoxygenase. The accuracy of a homology model built depends strongly on the degree of homology with the template sequence. The homology modeling methodology we used here for constructing the human 12S-LOX model may be adequate because the model is based on a sequence homology of 63% with the template (Rabbit 1LOX). In case of 12R-LOX, however, the sequence homology with template (Rabbit 1LOX) is only 33%. Despite this low sequence identity the model generated may be reasonable because the conservation in the iron-binding residues, position specific residues and stereo specific residues were taken into account during the construction of the model. The stereochemical quality of the model was validated using Procheck and Profile-3D. In the Ramachandran plot of 12R-LOX only seven residues (1.2%) were in the disallowed region where as 78.3% were in the most favored region, which shows that the quality of the model is good and can be considered for further studies. The overall folding pattern in the 12R-LOX and the 12S-LOX models is conserved with the available 3D structures of lipoxygenases. The large insertion is located beyond the N-terminal barrel at the start of the catalytic domain of the 12R-LOX and is accommodated on the outside of the protein without disruption of the overall tertiary structure. This extra sequence of the 12R-lipoxygenase was suggested to be involved in regulatory protein–protein interactions [8]. The 31-aa region contains a SH3-binding motif +XXPXXP where + is a positively charged amino acid, seven prolines and five arginines. The +XXPXXP motif seen is known to play an important role in protein–protein interactions [44].

The 12R and 12S-LOX active sites were then characterized from a structural point of view. The generated models obeyed the existing structural information on LOXs, such as alignment of substrate in the active site and position of iron atom in the active site. In the 12R-LOX arachidonic acid complex model it is observed that the arachidonic acid is in carboxylate end first orientation with the carboxyl group deep in the active site as proposed by Brash and co-workers [22]. This may explain the 10-fold higher activity of 12R-LOX reported at pH 6 (where the substrate is in uncharged state) when compared to pH 7.5 (where the substrate gets ionized) [21]. These uncharged molecules can easily reach into the hydrophobic LOX active site. It should be noted that our computational result is highly unanimous with their mutational result. Site-directed mutagenesis data on 12R-LOX proved the involvement of Gly441 in the enantioselectivity of the enzyme [23]. Brash et al. suggested that the Ala residue promotes oxygenation on the reactive pentadiene at the end deep in the substrate-binding pocket forming S hydroperoxide, and a Gly residue promotes oxygenation at the proximal end of the reactive pentadiene resulting in R stereochemistry [21–24]. In our studies we observed that the active site of 12R-LOX shows pocket near the Gly441 residue, which may be the potential oxygen-binding pocket. Results in docked poses are consistent with published mutation studies. C10 of the arachidonic acid is located in the open position of the coordination sphere such that oxygen is positioned closer to the Gly441 residue for attack at C-12. Ala403 is the corresponding residue of 12S-LOX to the Gly441 of 12R-LOX. In 12S-LOX, with the carboxylate end orientation of arachidonic acid it is observed that the oxygen-binding pocket is not seen near Ala. As noted, the Ala or Gly residue is situated near the entrance to the active site. In R-LOX, as the Gly is smaller the oxygenation on the near side of the pentadiene is favored to generate products with R specificity. In S-LOX, however, the larger Ala takes up space, causing oxygenation deeper in the pocket and thus generates the products with S stereospecificity. The substrate orientation is tail first in 12S-LOX which facilitates the oxygenation of C12 deeper in the pocket. These 12-LOX models thus support the theory of head to tail orientation [24]. The knowledge obtained on the 12R-LOX and 12S-LOX models, will permit detailed understanding of the active site geometry and the orientation of different amino acids at the active site. Additionally, this information of the 3D structure of 12R-LOX makes it much simpler to perform mutagenesis experiments aimed at designing novel therapeutic agents.

5. Conclusions

The present study on 12R and 12S-LOX homology models showed a conservation of the overall protein structural topology with the other enzymes of the same family. The metal coordination geometry in the enzymes was found to be in accordance with what is observed in a number of experimentally determined lipoxygenases protein structures. A 31-aa region is present only in 12R-LOX. This region is proline rich and consists of PXXP motifs. The docking results obtained correlated well with the existing hypotheses. Our results also support the proposed head to tail orientation. The present study is a step towards characterization of 12R-LOX.

Acknowledgements

We thank Centre for Modelling, Simulation and Design (CMSD), University of Hyderabad for permitting us to use the SGI workstation and InsightII facilities. We duly acknowledge Council of Scientific and Industrial Research (CSIR), Govt. of India for providing senior research fellowship to P. Aparoy.

Appendix A. Supplementary data

Supplementary data associated with this article can be found, in the online version, at doi:10.1016/j.jmgm.2008.11.009.

References

[1] S. Yamamoto, Mammalian lipoxygenases: molecular structures and functions, Biochim. Biophys. Acta 1128 (1992) 117–131.
[2] H. Porta, M. Rocha-Sosa, Lipoxygenases in bacteria: a horizontal transfer event? Microbiology 147 (2001) 3199–3200.
[3] C. Schneider, D.S. Keeney, W.E. Boeglin, A.R. Brash, Detection and cellular localization of 12R-lipoxygenase in human tonsils, Arch. Biochem. Biophys. 386 (2001) 268–274.
[4] R.A. Dixon, R.E. Jones, R.E. Diehl, C.D. Bennet, S. Kargman, C.A. Rouzer, Cloning of the cDNA for human 5-lipoxygenase, Proc. Natl. Acad. Sci. U.S.A. 85 (1988) 416–420.
[5] T. Matsumoto, C.D. Funk, O. Radmark, J.O. Hoog, H. Jornvall, B. Samuelsson, Molecular cloning and amino acid sequence of human 5-lipoxygenase, Proc. Natl. Acad. Sci. U.S.A. 85 (1988) 26–30.
[6] C.D. Funk, L. Furci, G.A. FitzGerald, Molecular cloning, primary structure and expression of the human platelet/erythroleukemia cell 12-lipoxygenase, Proc. Natl. Acad. Sci. U.S.A. 87 (1990) 5638–5642.
[7] T. Izumi, S. Hoshiko, O. Radmark, B. Samuelsson, Cloning of the cDNA for human 12-lipoxygenase, Proc. Natl. Acad. Sci. U.S.A. 87 (1990) 7477–7481.
[8] W.E. Boeglin, R.B. Kim, A.R. Brash, A (12R)-lipoxygenase in human skin: mechanistic evidence, molecular cloning and expression, Proc. Natl. Acad. Sci. U.S.A. 95 (1998) 6744–6749.
[9] E. Sigal, C.S. Craik, R.A. Dixon, J.A. Nadel, Cloning and expression of human arachidonate 15-lipoxygenase, Trans. Assoc. Am. Phys. 102 (1989) 176–184.
[10] A.R. Brash, W.E. Boeglin, M.S. Chang, Discovery of a second 15S-lipoxygenase in humans, Proc. Natl. Acad. Sci. U.S.A. 94 (1997) 6148–6152.
[11] H. Kuhn, J. Barnett, D. Grunberger, P. Baeker, J. Chow, B. Nguyen, H. Bursztyn-Pettegrew, H. Chan, E. Sigal, Overexpression, purification and characterisation of human recombinant 15-lipoxygenase, Biochem. Biophys. Acta 1169 (1993) 80–89.

[12] A.W. Ford-Hutchinson, M. Gresser, R.N. Young, 5-Lipoxygenase, Annu. Rev. Biochem. 63 (1994) 383–417.
[13] S. Ylä-Herttuala, M.E. Rosenfeld, S. Parthasarathy, E. Sigal, T. Särkioja, J.L. Witztum, D. Steinberg, Gene expression in macrophage-rich human atherosclerotic lesions. 15-Lipoxygenase and acetyl low density lipoprotein receptor messenger RNA colocalize with oxidation specific lipid-protein adducts, J. Clin. Invest. 87 (1991) 1146–1152.
[14] P.M. Woollard, Stereochemical difference between 12-hydroxy-5,8,10,14-eicosatetraenoic acid in platelets and psoriatic lesions, Biochem. Biophys. Res. Commun. 136 (1986) 169–175.
[15] A.N. Baer, M.V. Klaus, F.A. Green, Epidermal fatty acid oxygenases are activated in non-psoriatic dermatoses, J. Invest. Dermatol. 104 (1995) 251–255.
[16] S. Hammarström, M. Hamberg, B. Samuelsson, E.A. Duell, M. Stawiski, J.J. Voorhees, Increased concentrations of nonesterified arachidonic acid, 12L-hydroxy-5,8,10,14-eicosatetraenoic acid, prostaglandin E2, and prostaglandin F2alpha in epidermis of psoriasis, Proc. Natl. Acad. Sci. U.S.A. 72 (1975) 5130–5134.
[17] Z. Yu, C. Schneider, W.E. Boeglin, A.R. Brash, Mutations associated with a congenital form of ichthyosis (NCIE) inactivate the epidermal lipoxygenases 12R-LOX and eLOX3, Biochim. Biophys. Acta 1686 (2005) 238–247.
[18] N. Epp, G. Fürstenberger, K. Müller, S. de Juanes, M. Leitges, I. Hausser, F. Thieme, G. Liebisch, G. Schmitz, P. Krieg, 12R-lipoxygenase deficiency disrupts epidermal barrier function, J. Cell Biol. 177 (2007) 173–182.
[19] S.T. Prigge, J.C. Boyington, B.J. Gaffney, L.M. Amzel, Structure conservation in Lipoxygenases: structural analysis of Soyabean Liopoxygenase-1 and modeling of human lipoxygenases, Protein 24 (1996) 275–291.
[20] R.C. Scarrow, M.G. Trimitsis, C.P. Buck, G.N. Grove, R.A. Cowling, M.J. Nelson, X-ray spectroscopy of the iron site in soybean lipoxygenase-1: changes in coordination upon oxidation or addition of methanol, Biochemistry 33 (1994) 15023–15035.
[21] G. Coffa, C. Schneider, A.R. Brash, A comprehensive model of positional and stereo control in lipoxygenases, Biochem. Biophys. Res. Commun. 338 (2005) 87–92.
[22] G. Coffa, A.N. Imber, B.C. Maguire, G. Laxmikanthan, C. Schneider, B.J. Gaffney, A.R. Brash, On the relationships of substrate orientation, hydrogen abstraction, and product stereochemistry in single and double dioxygenations by soybean lipoxygenase-1 and its Ala542Gly mutant, J. Biol. Chem. 280 (2005) 38756–38766.
[23] S. Meruvu, M. Walther, I. Ivanov, S. Hammarström, G. Fürstenberger, P. Krieg, P. Reddanna, H. Kuhn, Sequence determinants for the reaction specificity of murine (12R)-lipoxygenase: targeted substrate modification and site-directed mutagenesis, J. Biol. Chem. 280 (2005) 36633–36641.
[24] G. Coffa, A.R. Brash, A single active site residue directs oxygenation stereospecificity in lipoxygenases: stereocontrol is linked to the position of oxygenation, Proc. Natl. Acad. Sci. U.S.A. 101 (2004) 15579–15584.
[25] E. Hornung, S. Rosahl, H. Kühn, I. Feussner, Creating lipoxygenases with new positional specificities by site-directed mutagenesis, Biochem. Soc. Trans. 28 (2000) 825–826.
[26] P. Aparoy, R.N. Reddy, L. Guruprasad, M.R. Reddy, P. Reddanna, Homology modeling of 5-lipoxygenase and hints for better inhibitor design, J. Comput. Aided Mol. Des. 22 (2008) 611–619.
[27] V. Kenyon, I. Chorny, W.J. Carvajal, T.R. Holman, M.P. Jacobson, Novel human lipoxygenase inhibitors discovered using virtual screening with homology models, J. Med. Chem. 49 (2006) 1356–1363.
[28] M.V. Reddy, V.K. Billa, V.R. Pallela, M.R. Mallireddigari, R. Boominathan, J.L. Gabriel, E.P. Reddy, Design, synthesis, and biological evaluation of 1-(4-sulfamylphenyl)-3-trifluoromethyl-5-indolyl pyrazolines as cyclooxygenase-2 (COX-2) and lipoxygenase (LOX) inhibitors, Bioorg. Med. Chem. 16 (2008) 3907–3916.
[29] S.A. Gillmor, A. Villasenor, R. Fletterick, E. Sigal, M.F. Browner, The structure of mammalian 15-lipoxygenase reveals similarity to the lipases and the determinants of substrate specificity, Nat. Struct. Biol. 4 (1997) 1003–1009.
[30] INSIGHT II, 2000, Molecular Modeling Software, Accelrys, Inc., San Diego, USA.
[31] H.M. Berman, J. Westbrook, Z. Feng, G. Gilliland, T.N. Bhat, H. Weissig, I.N. Shindyalov, P.E. Bourne, The Protein Data Bank, Nucleic Acids Res. 28 (2000) 235–242.
[32] Homology user guide, Accelrys, Inc., San Diego, USA, 1999.
[33] U.C. Singh, P.K. Weiner, J.K. Caldwell, P.A. Kollman, 1986, AMBER version 3.0 University of California at San Francisco, San Francisco, CA.
[34] R.N. Reddy, R. Mutyala, P. Aparoy, P. Reddanna, M.R. Reddy, Computer aided drug design approaches to develop cyclooxygenase based novel anti-inflammatory and anti-cancer drugs, Curr. Pharm. Des. 13 (2007) 3505–3517.
[35] Profile-3D user guide, Accelrys, Inc., San Diego, USA, 1999.
[36] R.A. Laskowski, D.S. Moss, J.M. Thornton, Main-chain bond lengths and bond angles in protein structures, J. Mol. Biol. 231 (1993) 1049–1067.
[37] I.N. Shindyalov, P.E. Bourne, Protein structure alignment by incremental combinatorial extension (CE) of the optimal path, Protein Eng. 11 (1998) 739–747.
[38] T.A. Binkowski, S. Naghibzadeh, J. Liang, CASTp: Computed Atlas of Surface Topography of proteins, Nucleic Acids Res. 31 (2003) 3352–3355.
[39] G. Jones, P. Willett, R.C. Glen, A.R. Leach, R. Taylor, Development and validation of a genetic algorithm for flexible docking, J. Mol. Biol. 267 (1997) 727–748.
[40] S.T. Prigge, J.C. Boyington, M. Faig, K.S. Doctor, B.J. Gaffney, Structure and mechanism of lipoxygenases, Biochimie 79 (1997) 629–636.
[41] Y.Y. Zhang, B. Lind, O. Radmark, B. Samuelsson, Iron content of human 5-lipoxygenase, effects of mutations regarding conserved histidine residues, J. Biol. Chem. 268 (1993) 2535–2541.
[42] T. Hammerberg, Y.Y. Zhang, B. Lind, O. Radmark, B. Samuelsson, Mutations at the C-terminal isoleucine and other potential iron ligands of 5-lipoxygenase, Eur. J. Biochem. 230 (1995) 401–407.
[43] A.W. Ravna, M. Jaronczyk, I. Sylte, A homology model of SERT based on the $LeuT_{Aa}$ template, Bioorg. Med. Chem. Lett. 16 (2006) 5594–5597.
[44] B.K. Kay, M.P. Williamson, M. Sudol, The importance of being proline: the interaction of proline-rich motifs in signaling proteins with their cognate domains, FASEB J. 14 (2000) 231–241.